NIH Public Access
Author Manuscript
*Brain Res*. Author manuscript; available in PMC 2011 July 30.

Published in final edited form as:
*Brain Res*. 2010 July 30; 1346: 92–101. doi:10.1016/j.brainres.2010.05.057.

# DISTRIBUTION OF 5-HT$_{1B}$ AND 5-HT$_{1D}$ RECEPTORS IN THE INNER EAR

**Seong-Ki Ahn** and
Department of Otolaryngology, Gyeongsang National University, Jinju, Korea

**Carey D. Balaban**
Departments of Otolaryngology, Neurobiology, Communication Sciences & Disorders and Bioengineering University of Pittsburgh, Pittsburgh, PA, USA

## Abstract

Migraine and anxiety disorders are frequently co-morbid with balance disorders. This study examined the relative distribution of subtypes of serotonin (5-HT) receptor in the inner ear of monkeys and rats. Most vestibular ganglion cells were immunoreactive for 5-HT$_{1B}$ and 5-HT$_{1D}$ receptors in macaques and rats. In the inner ear, 5-HT$_{1B}$ and 5-HT$_{1D}$ receptor immunopositivity was associated with endothelial cells of the vestibular ganglion, spiral ganglion, vestibulocochlear nerve, spiral ligament and stria vascularis. It was noteworthy that 5-HT$_{1B}$ and 5-HT$_{1D}$ receptors are expressed in parallel sites in peripheral vestibular and trigeminal systems, which may be a factor underlying the efficacy of triptans in treating migraine and migrainous vertigo. Because the vestibular ganglion and trigeminal ganglion are both within the subarachnoid space, an interaction between 5-HT$_{1B}$ and TRPV1 receptors on blood vessel and ganglion cells may also contribute to the vasospasm and the comorbid headache, dizziness, nausea and vomiting that accompany subarachnoid hemorrhage.

### Keywords

Inner ear; serotonin receptors; migrainous vertigo; vestibular ganglion; subarachnoid space

## INTRODUCTION

There has been growing recognition of the profound co-morbidity of panic disorder with agoraphobia and balance disorders (Dieterich et al., 2001; Eckhardt-Henn et al., 2003; Furman and Jacob, 2001; Jacob et al., 1985; Jacob et al., 1989; Staab, 2000; Yardley et al., 2001), the co-morbidity of migraine with balance disorders (Furman et al., 2003; Neuhauser et al., 2001), an increased susceptibility to motion sickness in migraineurs (Drummond, 2005; Marcus et al., 2005) and the co-morbidity of migraine with anxiety disorders (Radat and Swendsen, 2004). In fact, migrainous vertigo has been recently cited as the second most frequent cause of recurrent vertigo after benign paroxysmal positional vertigo (Neuhauser, 2007).

Corresponding Author: Carey D. Balaban, PhD, Department of Otolaryngology, University of Pittsburgh School of Medicine, 107 Eye & Ear Institute, 203 Lothrop Street, Pittsburgh, PA 15213 USA, Tel: 1-412-647-2298, Fax: 1-412-647-8720, cbalaban@pitt.edu.

**Publisher's Disclaimer:** This is a PDF file of an unedited manuscript that has been accepted for publication. As a service to our customers we are providing this early version of the manuscript. The manuscript will undergo copyediting, typesetting, and review of the resulting proof before it is published in its final citable form. Please note that during the production process errors may be discovered which could affect the content, and all legal disclaimers that apply to the journal pertain.

NIH-PA Author Manuscript
NIH-PA Author Manuscript
NIH-PA Author Manuscript

NIH-PA Author Manuscript

NIH-PA Author Manuscript

NIH-PA Author Manuscript

Four recent findings are consistent with the concept that, as in the case of trigeminal pathways in migraine, both peripheral and central vestibular mechanisms may contribute to co-morbid migraine and balance disorders (Furman et al., 2003; Furman et al., 2005).. Firstly, Drummond (Drummond, 2002) reported that trigeminal pain, pain sensitivity in the fingers and photophobia are augmented in migraineurs by simultaneous optokinetic stimulation motion. Secondly, he reported that motion sickness is augmented by simultaneous painful trigeminal stimulation in migraineurs (Drummond and Granston, 2004). Thirdly, Marano (Marano et al., 2005) reported that painful trigeminal stimulation has significant effects on nystagmus in migraine patients. Fourthly, the antimigraine drug rizatriptan (5-$HT_{1B}$ and $_{1D}$ receptor agonist) is efficacious against motion sickness in migraineurs (Marcus and Furman, 2006). Finally, we demonstrated in a murine neurogenic migraine model that peripheral serotonin administration elicits extravasation of protein in the inner ear, concomitant with extravasation in meninges and other perivascular regions (Koo and Balaban, 2006). These findings raise the possibility that central and peripheral serotonergic mechanisms in vestibular pathways may contribute to balance and migraine disorders.

The triptans that have anti-migraine efficacy (e.g., rizatriptan) have greatest affinity for 5-$HT_{1B}$ and 5-$HT_{1D}$ receptors, but also have a reasonably strong affinity for 5-$HT_{1A}$ receptors (Napier et al., 1999; Tfelt-Hansen et al., 2000). In contrast to the known association of these receptors with nociceptive trigeminal mechanisms, there is very limited information regarding the localization of serotonin receptors in the vestibular and auditory periphery. Oh et al. (Oh et al., 1999) identified mRNA for a variety of serotonin receptors in cochlear tissues, including 5-$HT_{1A,}$ 5-$HT_{1B}$, 5-$HT_{2B}$, 5-$HT_{2C}$, 5-$HT_{3}$, 5-$HT_{5B}$ and 5-$HT_{6}$. This study examines the distribution of immunoreactivity for 5-$HT_{1B}$ and 5-$HT_{1D}$ receptors in the inner ear of rats and monkeys. We suggest that parallel expression patterns of receptor expression in the trigeminal ganglion and vestibular ganglion may contribute to the widespread comorbidity of headache and dizziness in clinical conditions such as migrainous vertigo, mild traumatic brain injury and subarachnoid hemorrhage.

## RESULTS

### Western blots

The 5-$HT_{1B}$ receptor antibody recognizes a single 60–61 kDa band in Western blots of P1 and P2 fractions from rat whole brain and rhesus monkey medulla oblongata (Figure 1). The 5-$HT_{1D}$ receptor antibody recognizes a primary band at ~35 kDa in P1 and P2 centrifugation fractions from rat whole brain and monkey medulla oblongata, and additional higher molecular weight bands at 55–62 kDa and ~80 kDa. This is consistent with previous reports of both oligomer and heteromer formation (Lee et al., 2000) and the existence of multiple isoforms (Harriott and Gold, 2008).

### 5-HT receptor subtype expression in the vestibular and auditory periphery

**Monkeys—**Serotonin 5-$HT_{1B}$ and 5-$HT_{1D}$ receptor expression was associated strongly with vestibular ganglion cells (Figure 2) in both the inferior and superior vestibular ganglia. By contrast, relatively few spiral ganglion cells in the same temporal bone sections displayed significant 5-$HT_{1B}$ or 5-$HT_{1D}$ receptor immunoreactivity (Figure 3). Intense 5-$HT_{1B}$ receptor immunoreactivity was associated with blood vessels, particularly in the vestibular ganglion (Figure 2, arrows in upper panel). Most vestibular ganglion cells were immunopositive for either 5-$HT_{1B}$ (96% of the sample above background criterion, 91% of the sample with two standard deviations of immunonegative cell criterion) or 5-$HT_{1D}$ (87% of the sample; 86% of the sample with two standard deviations of immunonegative cell criterion) receptors in sections stained with a single antibody, suggesting that at least 78% of

NIH-PA Author Manuscript

NIH-PA Author Manuscript

NIH-PA Author Manuscript

the vestibular ganglion cells are immunoreactive for both proteins (by the most conservative criterion). The further analyses used the background criterion. The size distribution of these ganglion cells (square root of soma area in microns) was not fitted by a single Normal distribution (Kolmogorov-Smirnov test = 0.04, $p<0.001$ and Shapiro-Wilk test = 0.99, $p<0.001$), but could be described as a mixture of two normally distributed (Gaussian) populations with 70.4% of the observations from a 29.3 ± 5.6 (S.D) micron population and 29.6% of the cells from a 40.4 ± 6.4 micron population. The intensity of neuronal somatic immunoreactivity for both receptor types is shown in a histogram (Figure 4A) and normal probability plot (Figure 4B), which illustrate several features of interest. Firstly, the intensity of the 5-$HT_{1B}$ receptor reaction in immunopositive cells tended to be greater than the intensity of 5-$HT_{1D}$ receptor reaction in immunopositive cells. This difference was statistically significant by either parametric (separate variance $t = 18.9$, 1280.7 df, $p<0.001$) or nonparametric (Mann-Whitney U Chi-square approximation = 260.6, 1 df, -< 0.001). Secondly, ganglion cells with the greatest 5-$HT_{1B}$ receptor immunoreactivity intensity tended to be larger than less immunoreactive ganglion cells. As shown in Figure 4C–D, ganglion cells with immunoreaction intensities below the 90$^{th}$ quartile showed the same distribution as immunonegative cells and the mean cell diameters (square root area/pi) did not differ significantly from the immunonegative cells (LSD tests, not significant). However, the upper 10$^{th}$ quartile of cells in terms of 5-$HT_{1B}$ receptor immunoreactivity intensity included only a few larger ganglion cells; the mean diameter of these cells was significantly smaller than either of the latter groups with less intense immunoreactivity (LSD tests or Mann-Whitney U tests, $p<0.01$ versus lower 90$^{th}$ quantile). No cell size relationship was observed for 5-$HT_{1D}$ immunoreactive neurons.

**Rats—**Serotonin receptor expression was associated with both neurons and endothelial cells in the inner ear. Most ganglion cells in the vestibular ganglion showed immunoreactivity for 5-$HT_{1A}$ (Figure 5A), 5-$HT_{1B}$ (Figure 5B) and 5-$HT_{1D}$ receptors (Figure 5C). Strongly immunoreactive fibers extended into the central portion of the vestibular nerve; particularly for fibers expressing 5-$HT_{1A}$ receptors (Figure 5A). The staining of the ganglion cell bodies was homogeneous in frozen sections of ganglia extracted with the brain (Figure 5), but was more punctuate and associated with the cell membrane in paraffin sections of decalcified temporal bones (Figures 6–7). The quantitative data regarding reaction intensities in vestibular ganglion cells are summarized in Figure 8. The size distribution of these ganglion cells (diameter in microns) was fitted by a single Normal distribution (Kolmogorov-Smirnov test, $p>0.39$ and Shapiro-Wilk test, $p>0.24$), with a mean size of 18.4 ± 3.6 (S.D) microns. As in the monkey specimens, the vast majority of vestibular ganglion cells were immunopositive for either 5-$HT_{1B}$ (95.0% by background criterion, 94.0% by immunonegative population 2 standard deviation criterion) or 5-$HT_{1D}$ receptor protein (90.6% by background criterion, 83.5% by immunonegative population 2 standard deviation criterion) in sections stained with a single antibody, suggesting that at least 86% of the ganglion cells co-express the receptor subtypes. The intensity of neuronal somatic immunoreactivity for both receptor types is shown in a histogram (Figure 8A) and normal probability plot (Figure 8B). As observed in monkey temporal bone sections, the intensity of the 5-$HT_{1B}$ receptor reaction in immunopositive cells tended to be greater than the intensity of 5-$HT_{1D}$ receptor reaction in immunopositive cells. This difference was statistically significant by either parametric (separate variance $t = 9.4$, 539.3 df, $p<0.001$) or nonparametric (Mann-Whitney U Chi-square approximation = 83.7, 1 df, -< 0.001). Unlike the monkey findings, ganglion cells with the greatest intensity of 5-$HT_{1D}$ receptor immunoreactivity tended to be larger than less immunoreactive ganglion cells, while there was no cell size difference as a function of the intensity of the 5-$HT_{1B}$ immunoreaction. As shown in Figure 8C and E, ganglion cells with 5-$HT_{1D}$ receptor immunoreactivity intensities below the 90$^{th}$ quartile showed the same distribution as immunonegative cells and the mean

NIH-PA Author Manuscript

NIH-PA Author Manuscript

NIH-PA Author Manuscript

cell diameters did not differ significantly from the immunonegative cells (LSD tests, not significant). However, the upper 10$^{th}$ quartile of cells in terms of 5-HT$_{1D}$ receptor immunoreactivity intensity included only a few larger ganglion cells; the mean diameter of these cells was significantly smaller than either of the latter groups with less intense immunoreactivity (LSD tests, $p<0.01$ versus lower 90$^{th}$ quantile and immunonegative cells). No significant cell size relationship was observed for the intensity of 5-HT$_{1D}$ immunoreactivity in rat vestibular ganglion neurons (Figure 6D).

In addition to their distribution in vestibular ganglion cells, both 5-HT$_{1B}$ (Figure 5) and 5-HT$_{1D}$ receptor (Figure 6) immunopositive puncta and linear segments were associated with endothelial cells of small blood vessels in the vestibular ganglion and nerve, particularly within the bony labyrinth. Punctate and linear structures associated with endothelial cells in both the spiral ligament deep to the spiral prominence and the stria vascularis also displayed prominent 5-HT$_{1B}$ (Figure 4) and 5-HT$_{1D}$ receptor (Figure 5) immunoreactivity. Immunoreactivity was also associated with endothelial cells on blood vessels along the margins of the spiral ganglion (e.g., Figure 5).

## Discussion

The complexity of interactions between 5-HT$_{1A}$, 5-HT$_{1B}$ and 5-HT$_{1D}$ autoreceptors and heteroceptors has been discussed extensively in relation to the actions of antidepressant drugs, including selective serotonin reuptake inhibitors (SSRIs), in the central nervous system (Stamford et al., 2000). These interactions have been implicated in phenomena as diverse as anxiety, stress responses, spatial memory, cognitive responses to complexity, and migraine, and are often invoked in explaining the efficacy of drugs such as SSRIs and. triptans. Therefore, the fact that neurons in the inner ear show a repertoire of expression similar to structures such as the trigeminal ganglion and dorsal root ganglia suggests that there may be a unifying explanation for the efficacy of serotonergic medications in co-morbid balance disorders, anxiety disorders and migraine.

One interesting finding is that different sensory ganglia appear to have similar repertoires of serotonin receptor expression. Like trigeminal and dorsal root ganglia (Hou et al., 2001; Ma et al., 2001; Potrebic et al., 2003; Smith et al., 2002; Wotherspoon and Priestley, 2000), the vestibular and spiral ganglia in both monkeys and rats included neurons that were immunopositive for 5-HT$_{1B}$ and 5HT$_{1D}$ receptors. The 5-HT$_{1B}$ and 5HT$_{1D}$ receptor immunoreactivity in the trigeminal ganglion is associated primarily with small to medium sized ganglion cells, with relatively little expression by large ganglion cells. By contrast, the vast majority of vestibular ganglion cells (97% in monkeys and 95% in rats) were immunopositive for 5-HT$_{1B}$ receptors and similar proportions (87% in monkeys and 91% in rats) were immunopositive for 5HT$_{1D}$ receptors. These data indicate that at least 83% of the neurons in monkeys and at least 86% of the neurons in rats co-express the two receptors. The presence of 5-HT$_{1B}$ and 5HT$_{1D}$ receptor immunoreactivity was independent of vestibular ganglion cell size, which corresponds to the size range of small to medium sized trigeminal ganglion cells. Further, the high level of expression raises the likelihood that many of the TRPV1-immunopositive vestibular ganglion cells (Balaban et al., 2003; Kitahara et al., 2005) also express 5-HT$_{1B}$ and 5HT$_{1D}$ receptors.

The ligand binding based classification of 5-HT$_{1B}$ and 5-HT$_{1D}$ receptor subtypes in rats and humans was originally the source of controversy(Barnes and Sharp, 1999; Hartig et al., 1996), with the former subtype identified as the dominant form in rodents and the latter in other species Based upon gene sequence homologies, though, the nomenclature was modified more than a decade ago to equate the rat 5-HT$_{1B}$ receptor with the former human 5-HT$_{1D\beta}$ receptor and the rat 5-HT$_{1D}$ receptor with the former human 5-HT$_{1D\alpha}$

NIH-PA Author Manuscript

NIH-PA Author Manuscript

NIH-PA Author Manuscript

receptor(Barnes and Sharp, 1999; Hartig et al., 1996). In light of the history of the receptor nomenclature, it is of interest that there was a species difference in terms of the association of intense immunostaining with smaller vestibular ganglion cells. In monkeys, the most intense 5-$HT_{1B}$ receptor immunoreaction was associated with smaller vestibular ganglion cells with no association between the intensity of 5-$HT_{1D}$ receptor immunoreactivity and ganglion cell size. The converse was found in rats the most intense 5-$HT_{1D}$ receptor was associated with smaller vestibular ganglion cells, with no association between the intensity of 5-$HT_{1B}$ receptor immunoreactivity and ganglion cell size. The interpretation of the significance of the co-variation in distribution of 5-$HT_{1B}$ and 5-$HT_{1D}$ receptor protein is complicated by evidence that 5-$HT_{1B}$ and 5-$HT_{1D}$ receptors form homodimers when expressed alone and can form heterodimers when co-expressed in vitro (Xie et al., 1999). These 5-$HT_{1B}$/5-$HT_{1D}$ heterodimers show binding kinetics that are intermediate to the homodimeric 5-$HT_{1B}$ and 5-$HT_{1D}$ receptors (Xie et al., 1999). However, the high prevalence of 5-$HT_{1B}$ and 5$HT_{1D}$ receptor expression by vestibular ganglion cells in both monkeys and rats suggests a prominent role in afferent transmission.

Within the inner ear, the 5-$HT_{1B}$ and 5-$HT_{1D}$ receptors were associated with varicose and linear structures along endothelial cells in two regions of the spiral ligament (deep to the spiral prominence and stria vascularis) that show evidence of protein extravasation in an intravenous serotonin infusion model of migraine (Koo and Balaban, 2006). These receptor subtypes were also distributed on blood vessels associated with the vestibular ganglion and vestibular nerve and the margin of spiral ganglion. This localization of protein is consistent with a previous report of messenger RNA for 5-$HT_{1B}$ receptors in the lateral wall of mouse cochlea (Oh et al., 1999). Because the trigeminal ganglion provides sensory innervation to the vertebrobasilar, anterior inferior cerebellar and labyrinthine arteries (Vass et al., 1998; Vass et al., 2004), it seems likely that vascular innervation is associated with axons originating in 5-$HT_{1B}$ and 5-$HT_{1D}$ receptor immunopositive cell bodies in the trigeminal ganglion (Hou et al., 2001; Ma et al., 2001; Smith et al., 2002; Wotherspoon and Priestley, 2000).

The main finding of this study is that macaque and rat inner ear show robust distributions of 5-$HT_{1B}$ and 5-$HT_{1D}$ receptor expression. This finding is of interest because an effective class of anti-migraine drugs, the triptans, have greatest affinity for 5-$HT_{1B}$ and 5-$HT_{1D}$ receptors, but also have a reasonably strong affinity for 5-$HT_{1A}$ receptors (Napier et al., 1999; Tfelt-Hansen et al., 2000) and 5-$HT_{1F}$ receptors (Wood, 2002). The peripheral anti-migraine effects of triptans include selective constriction of pain-producing intracranial extracerebral blood vessels, reduction of trigeminal sensory nerve activation and inhibition of vasoactive neuropeptide release and inhibition of neurotransmitter release from activated trigeminal nerves in the brainstem and upper cervical spinal column (Goadsby et al., 2002; Silva et al., 2006).. Thus, in addition to binding to vascular serotonin receptors, it seems likely that the effects of triptans on 5-$HT_{1B}$ and 5-$HT_{1D}$ receptors have the likelihood of exerting multiple influences on vestibular information processing, particularly in patients with migrainous vertigo.

The parallel distributions of 5-$HT_{1B}$ and 5-$HT_{1D}$ receptor expression in the inner ear and trigeminal ganglion are also germane to the emerging interest in mechanisms underlying acute and delayed effects of subarachnoid hemorrhage (Macdonald et al., 2007; Sehba and Bederson, 2006). Effects of subarachnoid hemorrhage in the inner ear have been described previously (Schuknecht, 1974). The membranous labyrinth is a specialized endolymph-filled structure that is surrounded by a perilymph-filled extension of the subarachnoid space. The perilymph is confluent with the cerebrospinal fluid in the subarachnoid space through the cochlear aqueduct and it communicates freely with the interstitial spaces around the sensory hair cells and the ganglion cells. This relationship is analogous to the location of the

NIH-PA Author Manuscript

NIH-PA Author Manuscript

NIH-PA Author Manuscript

trigeminal ganglion in a pocket of subarachnoid space within the Meckel cave (Janjua et al., 2008). Like the trigeminal ganglion, the blood supply of these 'subarachnoid' inner ear structures is derived from the cerebral circulation. The labyrinthine artery emerges from either the basilar artery or the anterior inferior cerebellar artery, supplies the dura mater and nerves within the internal acoustic canal, then distributes to the membranous labyrinth via branches of the common cochlear artery (main cochlear, vestibulo-cochlear and posterior vestibular arteries) and the anterior vestibular artery (Schuknecht, 1974). Hence, both the neurons and blood vessels of the trigeminal ganglion and the inner ear can be influenced directly by molecules in the surrounding cerebrospinal fluid.

Subarachnoid hemorrhage produces acute increases in concentrations of both serotonin and 20-hydroxyeiscosatetraenoic acid (20-HETE, an arachidonic acid metabolite) in the cerebrospinal fluid, which produce a drop in regional cerebral blood flow by synergistic vasoconstrictor actions involving 5-$HT_{1B}$ receptors and direct responses to 20-HETE (Cambj-Sapunar et al., 2003). A delayed up-regulation of both 5-$HT_{1B}$ and endothelin 1 receptors also may contribute to increased susceptibility to delayed vasospasm after subarachnoid hemorrhage (Ansar et al., 2007; Hansen-Schwartz, 2004). These responses are very similar to the myogenic vasoconstriction that has been described in the rat mesenteric resistance arteries: a release of 20-HETE during elevated arterial transluminal pressure activates TRPV1 receptors on arterial terminals and vasoactive peptide release to produce a neurally-enhanced vasoconstriction (Scotland et al., 2004). Our data raise the hypothesis that similar vascular responses could occur in the inner ear small resistance arteries in scenarios ranging from normal blood flow autoregulation to pathological conditions such as subarachnoid hemorrhage (e.g., in head trauma). It further seems likely that serotonin and 20-HETE can contribute in a parallel manner to sensory symptoms via actions at both 5-$HT_{1B}$ and TRPV1 receptors expressed by the vestibular and spiral ganglion neurons (Balaban et al., 2003; Kitahara et al., 2005) and by trigeminal ganglion neurons (Hou et al., 2001; Ma et al., 2001; Price and Flores, 2007; Wotherspoon and Priestley, 2000). Hence, they may provide a target for intervention for co-morbid trigeminal and balance symptoms in the clinical setting.

## EXPERIMENTAL PROCEDURE

### Animals and tissue preparation

**Monkeys—**Decalcified Temporal bone sections from 5 macaques were used. The animals had been euthanized with pentobarbital sodium and perfused transcardially with phosphate buffer saline (pH 7.2–7.4), followed by either 4% paraformaldehyde in phosphate buffered saline or paraformaldehyde-lysine-sodium metaperiodate (PLP) fixative. The temporal bones were decalcified in 10% formic acid then neutralized overnight in 5% sodium sulfite by standard methods (Balaban et al., 2003) prior to trimming and paraffin embedding. The tissues were sectioned at 8–10 microns in the midmodiolar plane.

**Rats—**A total of 10 adult male Long-Evans rats (260–400 g; Charles River Laboratories, Wilmington, MA, USA) were used. The rats were deeply anesthetized with sodium pentobarbital (100 mg/kg, i.p.) and perfused transcardially with phosphate-buffered saline (PBS, 0.9% NaCl in 50 mM phosphate buffer, pH 7.3) followed by paraformaldehyde-lysine-periodate (PLP) fixative. The heads were removed, skinned and then the brains were carefully removed and placed in 30% sucrose-PBS at 4 °C for 48–72 h. Thirty five-micrometer sections were cut on a freezing-slide microtome, and sets of every six sections were collected in PBS containing 30% sucrose and 30% ethylene glycol and stored at −20 °C prior to immunohistochemistry. The temporal bones were post-fixed in 4% paraformaldehyde for at least 24 hrs at 22°C. The temporal bones were decalcified in 10%

NIH-PA Author Manuscript

NIH-PA Author Manuscript

NIH-PA Author Manuscript

formic acid then neutralized overnight in 5% sodium sulfite by standard methods (Balaban et al., 2003) prior to trimming and paraffin embedding. Paraffin embedded sections were cut with a microtome at 8 μm and mounted on subbed slides. The sections were then stored at 22°C prior to immunohistochemistry.

### Immunohistochemical procedures

All procedures were carried out at room temperature unless otherwise noted. For the rat brain tissues, after washing with distilled water (4×5 min), free-floating sections were incubated for 10 min with 0.9% $H_2O_2$ in PBS to remove endogenous peroxidase activity. After washing with distilled water and then with PBS, sections were treated for 1h with blocking buffer (PBS with 2% bovine serum albumin (BSA), and incubated for 48 h at room temperature in a rabbit polyclonal anti-5-$HT_{1A}$ receptor antibody (1:500; Immunostar Inc., Hudson, WI, USA), a rabbit polyclonal anti-5-$HT_{1B}$ receptor antibody (1:1,000; AB9401, Chemicon International, Temecula, CA, USA), and a rabbit polyclonal anti-5-$HT_{1D}$ receptor antibody (1:500–5,000; #71815, Imgenex, San Diego, CA, USA), respectively. Principles for development of these selective antibodies were described by Smith et al. (Smith et al., 1998). The polyclonal antibodies for the 5-$HT_{1B}$ and 5-$HT_{1D}$ receptors recognize specifically synthetic peptides corresponding to sequences from the third cytoplasmic domain of the respective human receptors, which are identical to the monkey sequence but each differ from the rat sequence in a single amino acid (BLAST search). These primary antisera were purified by antigen affinity chromatography. Western blots for brain fractions are shown in Figure 1. Control sections were stained by omitting the primary antibody. A preadsorbed control for 5-$HT_{1D}$ immunoreactivity, using a custom-synthesized lot of the oligopeptide antigen from Imgenex, eliminated immunoreactivity of the vestibular ganglion and cochlea in primate sections.

Following extensive washing with PBS to remove primary antisera, the sections were treated for 1 h with a biotinylated goat anti-rabbit antibody (1:100; Vector Laboratories, Burlingame, CA, USA) for 5-HT in PBS containing 2% BSA. After three washes with PBS, sections were incubated in avidin-biotin-peroxidase reagent (Vectastain ABC Elite Kit, Vector Laboratories) for 1 h, washed repeatedly with PBS, and transferred to 50 mM Tris buffer (pH 7.2) for 10 min. Immunoreactivity was then visualized by reaction with 3.3′-diaminobenzidine tetrahydrochloride (DAB) chromagen (8.3 μl, 30% H2O2 and 20 mg DAB in 100 ml of 0.5 M sodium acetate buffer, pH 6.0). The sections were rinsed with distilled water and mounted on gelatin/chrome alum-subbed slides. After air-drying overnight, the sections were dehydrated through a graded series of ethanol, cleared with xylene, and coverslipped with DPX Mountant (Fluka, Milwaukee, WI, USA).

For the embedded temporal bones, tissue sections were de-paraffinized. They were then heated for 20 minutes at 90–98°C in a low pH (3.0) sodium citrate-citric acid buffer (antigen retrieval) and rinsed thoroughly with PBS. The rest of the immunohistochemical procedures were identical to the protocol for free-floating sections.. Primary antibodies were omitted in the control sections. Stained sections were then dehydrated by increasing concentration of ethanol, treated with xylene and cover-slipped with Permount.

## Data analysis

Digital images of expressed the 5-HT receptors in temporal bone tissues were prepared using a Nikon Eclipse E600N microscope equipped with a Spot RT Monochrome camera (Model 2.1.1, Diagnostic instruments, Inc., Sterling Heights, MI, USA). The images were captured on a Pentium-based computer running Meta-Morph software (ver. 6.1r4, Universal Imaging Corporation, Downingstown, PA, USA). The staining density and somatic area of immunoreactive vestibular ganglion neurons were quantified from 12 bit digital images,

NIH-PA Author Manuscript

NIH-PA Author Manuscript

NIH-PA Author Manuscript

taken with a 40X objective. Somata containing nuclei and nucleoli were outlined manually in MetaMorph and statistics logged automatically. Regions containing no tissue (slide, coverslip and mounting media only) were measured as an absolute calibration zero for variations in optical transmission between the light source and the CCD element; they were subtracted from the data initially to normalize readings between slides. Control regions for background staining were assessed from the parenchyma of the ganglion and the peripheral nerve, which have at least the same baseline optical density as immunonegative neuronal cells bodies. These background readings were subtracted from the data. Hence, background staining appears predominantly as negative values in Figures 4 and 8. For monkeys, the zero value corresponds to a z-score of 0.90 for the 5-$HT_{1B}$ immunonegative population (96% of total cells are immunopositive) and. 1.68 for the 5-$HT_{1D}$ immunonegative population (87% of the total population are immunopositive). By a two standard deviation immunonegative population criterion (Price and Flores, 2007), 91% of the monkey vestibular ganglion cells were 5-$HT_{1B}$ immunopositive and 86% were 5-$HT_{1D}$ immunopositive.. Parallel analyses of the rat ganglion cells yielded estimates of 95.0% of vestibular ganglion cells immunopositive for 5-$HT_{1B}$ or 90.6% immunopostive for 5-$HT_{1D}$ receptor protein with the background criterion, versus 94% for the 5-$HT_{1B}$ receptor and 83.5% for the 5-$HT_{1D}$ receptor with a two standard deviation of the immunonegative population criterion. (SYSTAT 11 (SYSTAT Software, Inc,) was used for standard statistical analyses such as Wilk-Shapiro tests, Kolmolgov-Smirnov tests, Mann-Whitney U tests, Analysis of variance, least significant differences (LSD) tests, quantile plots and normal probability plots. The quantile and probability plots, Kolmogorov-Smirnov tests and Wilk-Shapiro tests were used to test conformity of data to assumptions about underlying normality and being identicallydistributed. Analysis of Variance with LSD tests and Mann-Whitney U tests were used to test specific hypotheses under assumptions of normality or identical underlying distributions, respectively. In addition, k-means cluster analysis (for initial estimates) were followed by order statistics approach to estimate the distribution of a data set as a mixture to two normal (Gaussian) populations, following procedures described for circular normal data in a previous publication (McCandless and Balaban, 2010). Adobe Photoshop 7.0 (Adobe system, Inc., San Jose, CA, USA) was used for brightness and contrast adjustment and cropping of photomicrographs for the illustrations.

## LITERATURE REFERENCES


Ansar S, Svendgaard NA, Edvinsson L. Neurokinin-1 receptor antagonism in a rat model of subarachnoid hemorrhage: prevention of upregulation of contractile $ET_B$ and 5-$HT_{1B}$ receptors and cerebral blood flow reduction. J Neurosurg. 2007; 106:881–886. [PubMed: 17542534]

Balaban CD, Zhou J, Li HS. Type 1 vanilloid receptor expression by mammalian inner ear ganglion cells. Hearing Research. 2003; 175:165–170. [PubMed: 12527134]

Barnes NM, Sharp T. A review of central 5-HT receptors and their function. Neurophamacology. 1999; 38:1083–1052.

Cambj-Sapunar L, Yu M, Harder DR, Roman RJ. Contribution of 5-hydroxytryptamine$_{1B}$ receptors and 20-hydroxyeiscosatraenoic acid to fall in cerebral blood flow after subarachnoid hemorrhage. Stroke. 2003; 34:1264–1275.

Dieterich M, Krafczyk S, Querner V, Brandt T. Somatoform phobic postural vertigo and psychogenic disorders of stance and gait. Advances in Neurology. 2001; 87:225–233. [PubMed: 11347225]

Drummond PD. Motion sickness and migraine: optokinetic stimulation increases scalp tenderness, pain sensitivity in the fingers and photophobia. Cephalagia. 2002; 22:117–124.

Drummond PD, Granston A. Facial pain increases nausea and headache during motion sickness in migraine sufferers. Brain. 2004; 127:526–534. [PubMed: 14749288]

Drummond PD. Triggers of motion sickness in migraine sufferers. Headache. 2005; 45:653–656. [PubMed: 15953297]

NIH-PA Author Manuscript

NIH-PA Author Manuscript

NIH-PA Author Manuscript

Eckhardt-Henn A, Breuer P, Thomalske C, Hoffmann SO, Hopf HC. Anxiety disorders and other psychiatric subgroups in patients complaining of dizziness. Journal of Anxiety Disorders. 2003; 17:369–388. [PubMed: 12826087]

Furman JM, Jacob RG. A clinical taxonomy of dizziness and anxiety in the otoneurologic setting. J Anxiety Disorders. 2001; 15:9–26.

Furman JM, Marcus DA, Balaban CD. Migrainous vertigo: development of a pathogenetic model and structured diagnostic interview. Curr Opin Neurology. 2003; 16:5–13.

Furman JM, Balaban CD, Jacob RG, Marcus DA. Migraine-anxiety associated dizziness (MARD): a new disorder? Journal of Neurology, Neurosurgery and Psychiatry. 2005; 76:1–8.

Goadsby PJ, Lipton RB, Ferrari MD. Drug therapy: migraine--current understanding and treatment. N Engl J Med. 2002; 346:257–270. [PubMed: 11807151]

Hansen-Schwartz J. Receptor changes in cerebral arteries after subarachnoid haemorrhage. Acta Neurol Scand. 2004; 109:33–44. [PubMed: 14653848]

Harriott AM, Gold MS. Serotonin type 1D receptors ($5HT_{1D}R$) are differentially distributed in nerve fibers innervating craniofacial tissues. Cephalalgia. 2008; 28:933–944. [PubMed: 18557979]

Hartig PR, Hoyer D, Humphrey PA, Martin GR. Alignment of receptor nomenclature with the human genome: classification of 5-$HT_{1B}$ and 5-$HT_{1D}$ receptor subtypes. Trends in Pharmcol Sci. 1996; 17:103–105.

Hou M, Kanje M, Longmore J, Tajti J, Uddman R, Edvinsson L. 5-$HT_{1B}$ and 5-$HT_{1D}$ receptors in the human trigeminal ganglion: co-localization with calcitonin gene-related peptide, substance P and nitric oxide synthase. Brain Res. 2001; 909:112–120. [PubMed: 11478927]

Jacob RG, Moller MB, Turner SM, Wall C. Otoneurological examination of panic disorder and agoraphobia with panic attacks: a pilot study. Am J Psychiat. 1985; 142:715–720. [PubMed: 3873876]

Jacob RG, Lilienfeld SO, Furman JMR, Durrant JD, Turner SM. Panic disorder with vestibular dysfunction: further clinical observations and description of space and motion phobic stimuli. J Anxiety Disorders. 1989; 3:117–130.

Janjua R, Al-Mefty O, Densler DW, Shields CB. Dural relationships of Meckel cave and lateral wall of the cavernous sinus. Neurosurg Focus. 2008; 25:E2. [PubMed: 19035700]

Kitahara T, Li HS, Balaban CD. Changes in transient receptor potential cation channel superfamily V (TRPV) mRNA expression in the mouse inner ear ganglia after kanamycin challenge. Hearing Research. 2005; 201:132–144. [PubMed: 15721568]

Koo JW, Balaban CD. Serotonin-induced plasma extravasation in the murine inner ear: possible mechanism of migraine-associated inner ear dysfunction. Cephalagia. 2006; 26:1310–1319.

Lee SP, Xie Z, Varghese G, Nguyen T, O'Dowd BF, George SR. Oligomerization of dopamine and serotonin receptors. Neuropsychopharmacology. 2000; 23:S32–S40. [PubMed: 11008065]

Ma QP, Hill RG, Sirinathsinghi D. Colocalization of CGRP with 5-HT1B/1D receptors and substance P in trigeminal ganglion neurons in rats. Eur J Neurosci. 2001; 13:2099–2104. [PubMed: 11422450]

Macdonald RL, Pluta RM, Zhang JH. Cerebral vasospasm after subarachnoid hemorrhage: the emerging revolution. Nature Clin Prac Neurol. 2007; 3:256–263.

Marano E, Marcelli V, Di Stasio E, Bonuso S, Vacca G, Manganelli F, Marciano E, Perretti A. Trigeminal stimulation elicits a peripheral vestibular imbalance in migraine patients. Headache. 2005; 45:325–331. [PubMed: 15836568]

Marcus DA, Furman JM, Balaban CD. Motion sickness in migraine sufferers. Expert Opinion in Pharmacotherapy. 2005; 6:2691–2697.

Marcus DA, Furman JM. Prevention of motion sickness with rizatriptan: a double-blind, placebo-controlled pilot study. Medical Science Monitor. 2006; 12:PI1–7. [PubMed: 16369474]

McCandless CH, Balaban CD. Parabrachial nucleus neuronal responses to off-vertical axis rotation in macaques. Exp Brain Res. 2010; 202:271–290. [PubMed: 20039027]

Napier C, Stewart M, Melrose H, Hopkins B, McHarg A, Wallis R. Characterization of the 5-HT receptor binding profile of eletriptan and kinetics of [$^3$H]eletriptan binding at human 5-$HT_{1B}$ and 5-$HT_{1D}$ receptors. Eur J Pharmacol. 1999; 368:259–268. [PubMed: 10193663]

NIH-PA Author Manuscript

NIH-PA Author Manuscript

NIH-PA Author Manuscript

Neuhauser H, Leopold M, von Brevern M, Arnold G, Lempert T. The interrelations of migraine, vertigo, and migrainous vertigo. Neurology. 2001; 56:436–441. [PubMed: 11222783]

Neuhauser HK. Epidemiology of vertigo. Curr Opin Neurology. 2007; 20:40–46.

Oh CK, Drescher MJ, Hatfield JS, Drescher DG. Selective expression of serotonin receptor transcripts in the mammalian cochlea and its subdivisions. Hearing Research. 1999; 70:135–40.

Potrebic S, Ahn AH, Skinner K, Fields HL, Basbaum AI. Peptidergic nociceptors of both trigeminal and dorsal root ganglia express serotonin 1D receptors: inplications for the selective antimigraine action of triptans. J Neurosci. 2003; 23:10988–10997. [PubMed: 14645495]

Price TJ, Flores CM. Critical evaluation of the colocalization between calcitonin gene-related peptide, Substance P, Transient Receptor Potential Vanilloid Subfamily Type 1 immunoreactivities and Isolectin $B_4$ binding in primary afferent neurons of the rat and mouse. J Pain. 2007; 8:263–272. [PubMed: 17113352]

Radat F, Swendsen J. Psychiatric morbidity in migraine: a review. Cephalagia. 2004; 25:165–178.

Schuknecht, HF. Pathology of the Ear. Harvard University Press; Cambridge, MA: 1974.

Scotland RS, Chauhan S, Davis C, De Filipe C, Hunt S, Kabir J, Kotsonis P, Oh U, Ahluwalia A. Vanilloid receptor TRPV1, sensory C-fibers, and vascular autoregulation: a novel mechanism involved in myogenic constriction. Circulation Res. 2004; 95:1027–1034. [PubMed: 15499026]

Sehba FA, Bederson JB. Mechanisms of acute brain injury after subarachnoid hemorrhage. Neurological Research. 2006; 28:381–398. [PubMed: 16759442]

Silva SA, Marques FB, Fontes Ribero CA. Characterization of the human basilar artery contractile response to 5-HT and triptans. Fundamental & Clinical Pharmacology. 2006; 21:265–272. [PubMed: 17521295]

Smith D, Shaw D, Hopkins R, McAllister G, Hill R, Sirinathsinghi D, Longmore J. Development and characterisation of human 5-$HT_{1B}$- or 5-$HT_{1D}$-receptor specific antibodies as unique research tools. J Neurosci Methods. 1998; 80:155–161. [PubMed: 9667388]

Smith D, Hill RG, Edvinsson L, Longmore J. An immunocytochemical investigation of human trigeminal nucleus caudalis: CGRP, substance P and 5-$HT_{1D}$-receptor immunoreactivities are expressed by trigeminal sensory fibres. Cephalagia. 2002; 22:424–431.

Staab JP. Diagnosis and treatment of psychological symptoms and psychiatric disorders in patients with dizziness and imbalance. Otolaryngologic Clinics of North America. 2000; 33:617–636. [PubMed: 10815040]

Stamford JA, Davidson C, McLaughlin DP, Hopwood SE. Control of dorsal raphe 5-HT function by multiple 5-HT1 autoreceptors: parallel purposes or plurality? TINS. 2000; 23:459–465. [PubMed: 11006462]

Tfelt-Hansen P, De Vries P, Saxena PR. Triptans in migraine: a comparative review of pharmacology, pharmacokinetics and efficacy. Drugs. 2000; 60:1259–1287. [PubMed: 11152011]

Vass Z, Shore SE, Nuttall AL, Miller JM. Direct evidence of trigeminal innervation of cochlear blood vessels. Neuroscience. 1998; 84:559–567. [PubMed: 9539226]

Vass Z, Dai CF, Steyger PS, Jancsó G, Trune DR, Nuttall AL. Co-localization of the vanilloid capsaicin receptor and substance P in sensory nerve fibers innervating cochlear and vertebro-basilar arteries. Neuroscience. 2004; 124:919–927. [PubMed: 15026132]

Wotherspoon G, Priestley JV. Expression of the 5-$HT_{1B}$ receptor by subtypes of rat trigeminal ganglion cells. Neuroscience. 2000; 95:465–471. [PubMed: 10658626]

Xie Z, Lee SP, O'Dowd BF, George SR. Serotonin 5-$HT_{1B}$ and 5-$HT_{1D}$ receptors form heterodimers when expressed alone and heterodimers when co-expressed. FEBS Letters. 1999; 456:63–67. [PubMed: 10452531]

Yardley L, Owen N, Nazareth I, Luxon L. Panic disorder with agoraphobia associated with dizziness: characteristic symptoms and psychosocial sequelae. Journal of Nervous & Mental Disease. 2001; 189:321–327. [PubMed: 11379977]

NIH-PA Author Manuscript

NIH-PA Author Manuscript

NIH-PA Author Manuscript

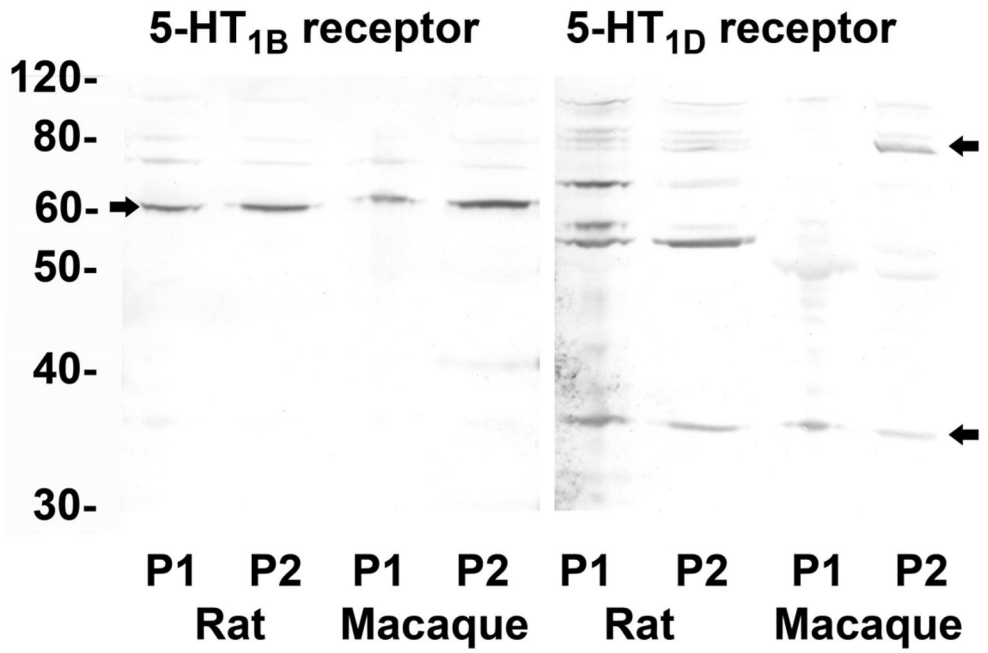


**Figure 1.**

Western blots. Proteins from P1 and P2 fractions of rat brain and monkey medulla oblongata were separated on a NuPAGE™ 10% Bis-Tris gel and blotted onto an Invitrolon™ PVDF membrane (Invitrogen). Binding of the primary antibody (1:1000 dilution) was detected with an alkaline phospatase-conjugated secondary antibody and histochemical substrate (WesternBreeze™, Invitrogen). The blot was digitized with a flatbed photo scanner (Epson V500). Arrows indicate major immunopositive bands in rats and monkeys mentioned in text.

NIH-PA Author Manuscript

NIH-PA Author Manuscript

NIH-PA Author Manuscript

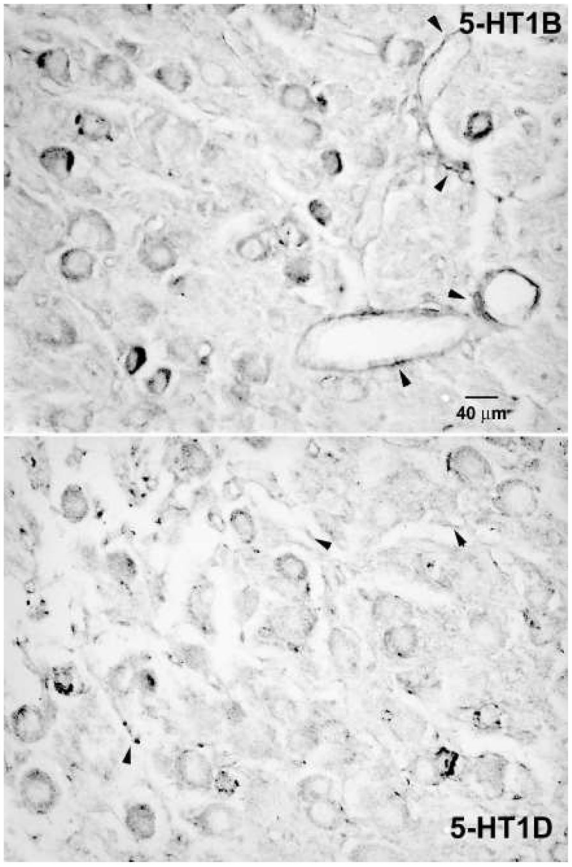


**Figure 2.**
Photomicrographs of the vestibular ganglion from decalcified, paraffin embedded monkey temporal bones. Vestibular ganglion cells showed expression of 5-$HT_{1B}$ (upper panel) and 5-$HT_{1D}$ (lower panel) immunoreactivity. Perivascular staining is indicated by small arrowheads.

NIH-PA Author Manuscript

NIH-PA Author Manuscript

NIH-PA Author Manuscript

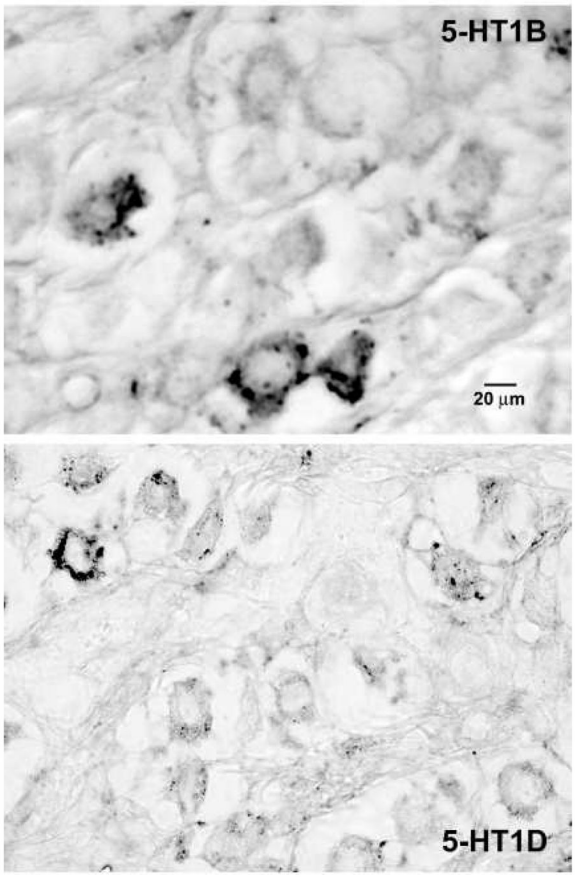


**Figure 3.**
Photomicrographs of spiral ganglion cells from decalcified, paraffin embedded monkey temporal bones. Representative images of 5-$HT_{1B}$ (upper panel) and 5-$HT_{1D}$ (lower panel) immunoreactivity illustrate that there were fewer intensely immunoreactive ganglion cells in the spiral ganglion than the vestibular ganglion, interspersed among many very lightly stained and immunonegative neurons.

NIH-PA Author Manuscript

NIH-PA Author Manuscript

NIH-PA Author Manuscript

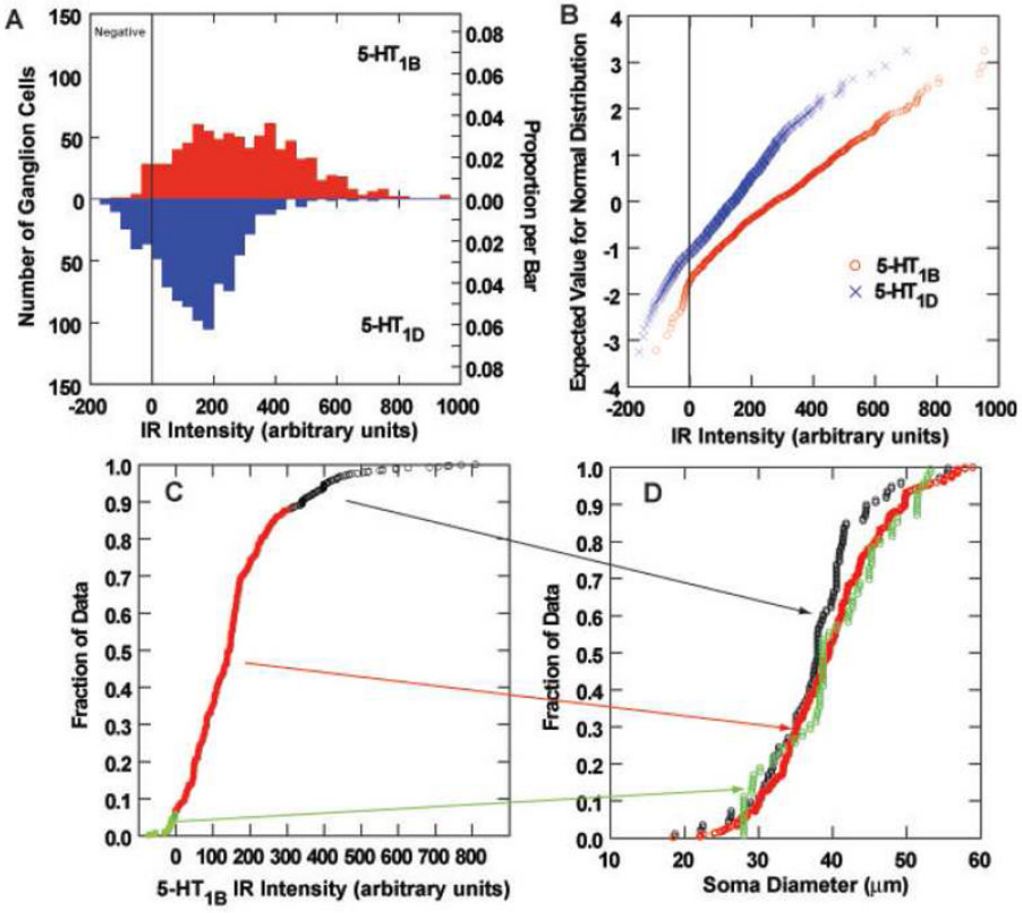


**Figure 4.**

Analysis of 5-$HT_{1B}$ and 5-$HT_{1D}$ immunoreactivity (IR) of monkey vestibular ganglion cells. A. Histograms of the distribution of 5-$HT_{1B}$ (upper panel) and 5-$HT_{1D}$ (lower panel) IR of vestibular ganglion cells. The demarcation between immunonegative and immunopositive data is shown by a vertical line. B. Full normal probability plots of the intensity data from panel A. The demarcation between immunonegative and immunopositive data is shown by a vertical line. C. The cumulative distribution curve for the intensity of 5-$HT_{1B}$ IR, with immunonegative cells plotted in green symbols, immunopositive cells below the $90^{th}$ percentile in intensity shown in red symbols, and the most intensely immunopositive cells (most intense 10%) plotted in black symbols. D. Cumulative distribution functions of soma sizes are shown for the three intensity populations identified in panel C. Note that the most intensely stained neurons tend to be smaller than less intensely IR or immunonegative vestibular ganglion cells.

NIH-PA Author Manuscript

NIH-PA Author Manuscript

NIH-PA Author Manuscript

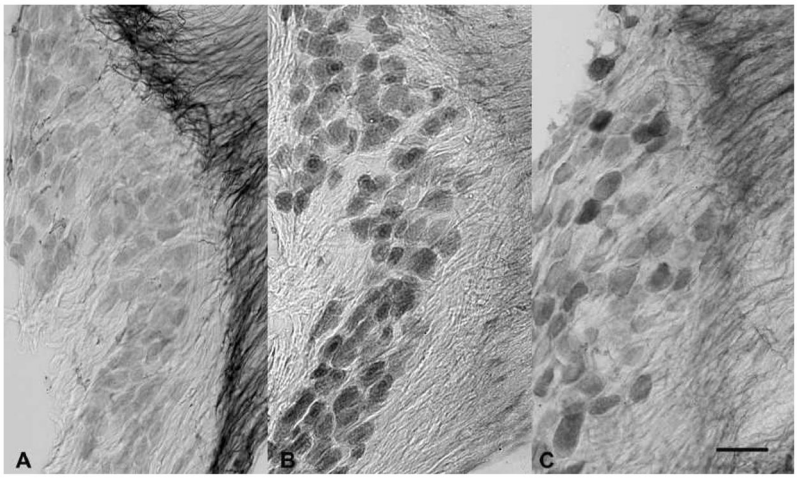


**Figure 5.**

Photomicrographs of the vestibular ganglion from frozen sections of ganglia extracted with the brain. Vestibular ganglion cells showed reasonably intense expression of 5-$HT_{1A}$ (photo A), 5-$HT_{1B}$ (photo B) and 5-$HT_{1D}$ (photo C) receptor immunoreactivity. Immunoreactive fibers extended into the central portion of the vestibular nerve. The calibration bar represents 50 μm.

NIH-PA Author Manuscript
NIH-PA Author Manuscript
NIH-PA Author Manuscript



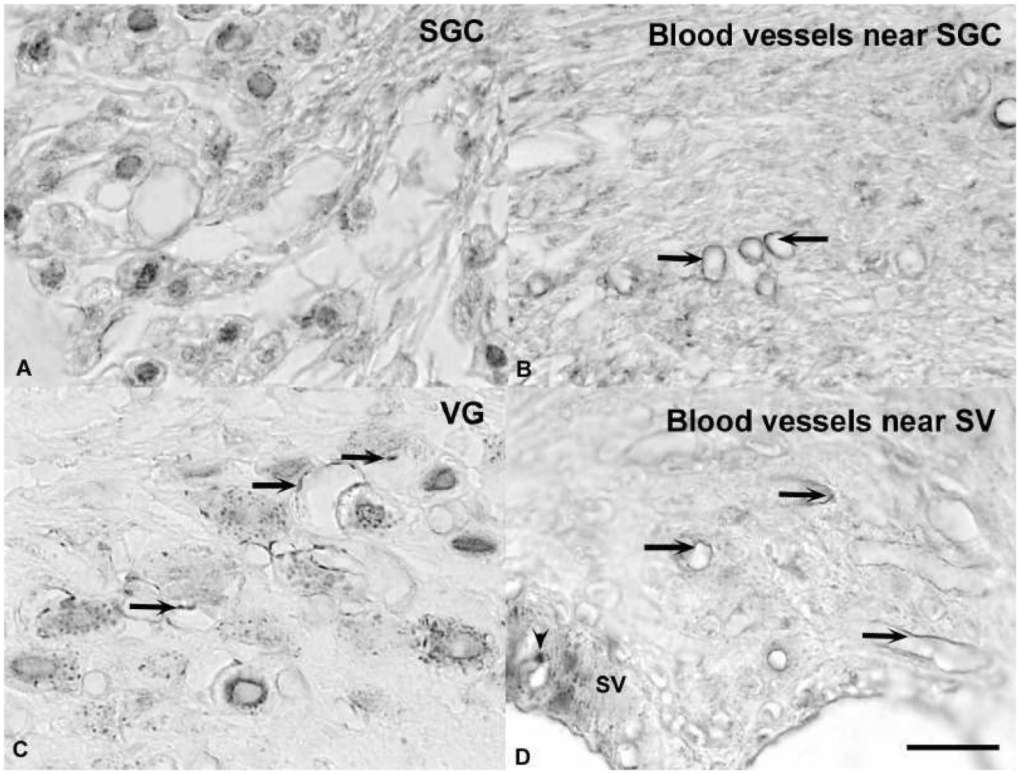


**Figure 6.**
Photomicrographs of 5-$HT_{1B}$ immunoreactivity in paraffin embedded, decalcified temporal bone sections. A. Spiral ganglion cells (SGC) showed punctuate immunoreactivity associated with the somatic cell membrane. B. Arrows show examples of both punctuate and linear immunopositivity that was associated with small blood vessels near the SGCs. C. Vestibular ganglion (VG) cells displayed punctuate somatic immunoreactivity. Arrows indicate immunoreactivity that was associated with blood vessels. D. Arrows show examples of both punctuate and linear immunopositivity that was associated with small blood vessels near the stria vascularis (SV). The plain arrowhead indicates a process of a melanocyte. The calibration bar represents 20 μm.

NIH-PA Author Manuscript
NIH-PA Author Manuscript
NIH-PA Author Manuscript



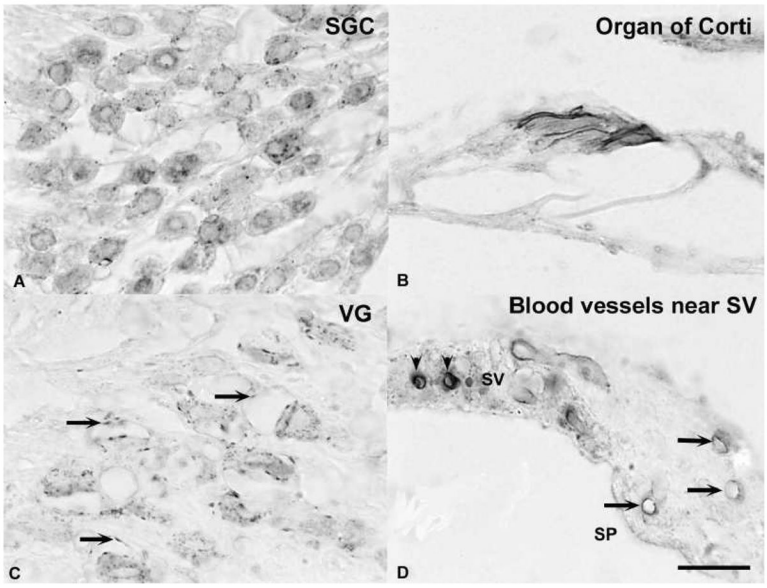


**Figure 7.**

Photomicrographs of 5-$HT_{1D}$ immunoreactivity in paraffin embedded decalcified temporal bone sections. A. Spiral ganglion cells (SGC) showed punctuate immunoreactivity associated with the somatic cell membrane. B. An intense immunoreaction was associated with the margin of outer hair cells in the organ of Corti.. C. Vestibular ganglion (VG) cells displayed punctuate somatic immunoreactivity. Arrows indicate immunoreactivity that was associated with blood vessels. D. Arrows show examples of both punctuate and linear immunopositivity that was associated with small blood vessels near the stria vascularis (SV). The plain arrowheads indicate SV melanocytes. The calibration bar represents 20 μm.

NIH-PA Author Manuscript

NIH-PA Author Manuscript

NIH-PA Author Manuscript

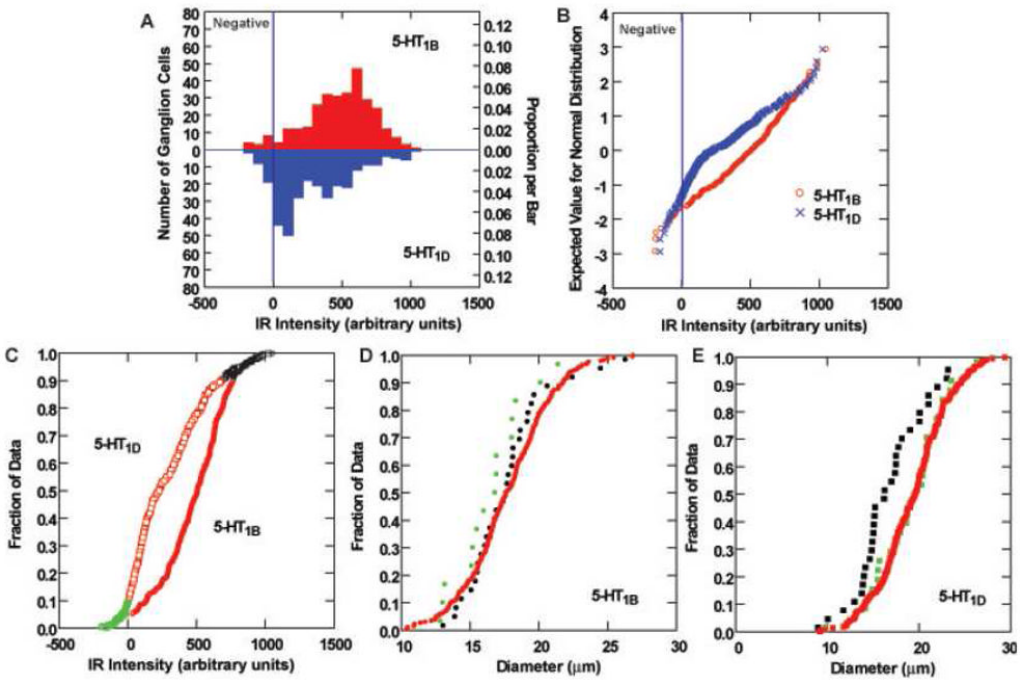


**Figure 8.**

Analysis of 5-$HT_{1B}$ and 5-$HT_{1D}$ immunoreactivity (IR) of rat vestibular ganglion cells. A. Histograms of the distribution of 5-$HT_{1B}$ (upper panel) and 5-$HT_{1D}$ (lower panel) IR of vestibular ganglion cells. The demarcation between immunonegative and immunopositive data is shown by a vertical line. B. Full normal probability plots of the intensity data from panel A. The demarcation between immunonegative and immunopositive data is shown by a vertical line. C. The cumulative distribution curve for the intensity of 5-$HT_{1B}$ IR, with immunonegative cells plotted in green symbols, immunopositive cells below the $90^{th}$ percentile in intensity shown in red symbols, and the most intensely immunopositive cells (most intense 10%) plotted in black symbols. D–E. Cumulative distribution functions of soma sizes are shown for the three intensity populations identified in panel C. There is association between intense 5-$HT_{1B}$ immunoreactivity and soma diameter (D). However, the most intensely 5-$HT_{1D}$ stained neurons (F) are smaller than less intensely IR or immunonegative vestibular ganglion cells.